Phase Behavior of Binary Blends of High Molecular Weight Diblock Copolymers with a Low Molecular Weight Triblock

Rafal A. Mickiewicz,[†] Eleftherios Ntoukas,[‡] Apostolos Avgeropoulos,[‡] and Edwin L. Thomas*,[†]

Department of Materials Science and Engineering, Massachusetts Institute of Technology, 77 Massachusetts Avenue, Cambridge, Massachusetts 02139, and Department of Materials Science and Engineering, University of Ioannina, University Campus−Dourouti, Ioannina 45110, Greece

Received October 17, 2007; Revised Manuscript Received June 11, 2008

ABSTRACT: Binary blends of four different high molecular weight poly(styrene-*b*-isoprene) (SI) diblock copolymers with a lower molecular weight poly(styrene-*b*-isoprene-*b*-styrene) (SIS) triblock copolymer were prepared, and their morphology was characterized by transmission electron microscopy and ultra-small-angle X-ray scattering. All the neat block copolymers have nearly symmetric composition and exhibit the lamellar morphology. The SI diblock copolymers had number-average molecular weights, $\bar{M}_n$, in the range $4.4 \times 10^5-1.3 \times 10^6$ g/mol and volume fractions of poly(styrene), Φ_{PS}, in the range 0.43−0.49, and the SIS triblock had a molecular weight of $\bar{M}_n \sim 6.2 \times 10^4$ g/mol with $\Phi_{PS} = 0.41$. The high molecular weight diblock copolymers are very strongly segregating, with interaction parameter values, χN, in the range 470−1410. A morphological phase diagram in the parameter space of molecular weight ratio ($R = M_n^{diblock}/{}^1/_2 M_n^{triblock}$) and blend composition was constructed, with R values in the range between 14 and 43, which are higher than previously reported. The phase diagram revealed a large miscibility gap for the blends, with macrophase separation into two distinct types of microphase-separated domains for weight fractions of SI, $w_{SI} < 0.9$, implying virtually no solubility of the much higher molecular weight diblocks in the lower molecular weight triblock. For certain blend compositions, above $R \sim 30$, morphological transitions from the lamellar to cylindrical and bicontinuous structures were also observed.

Introduction

Polymer-based materials are frequently comprised of different polymeric species blended together. Blending allows not only for a reduction in costs but also serves as an inexpensive and facile method to tune and manipulate the properties of the polymer system for a given application. Block copolymers are often used in blend systems as compatibilizers, since most polymers are immiscible.[1] Numerous studies have been undertaken on blends of block copolymers with homopolymers as well as block copolymers with other block copolymers.[2] In the latter category, the bulk of the work has been on blends of two diblock copolymers of moderate molecular weight (predominantly $\sim 1 \times 10^5$ g/mol). A series of publications by Hashimoto et al. examined the morphology and microphase separation behavior of blends of two A−B type diblock copolymers identical in chemical composition but varying in degree of polymerization and volume fraction of the respective blocks.[3−11] The blends displayed a rich variety of single microphase or macrophase separated morphologies, depending on blend composition (volume fraction of the respective diblocks), individual copolymer composition (volume fraction of the constituent blocks), and molecular weight ratio (R, defined as the ratio of the degree of polymerization of the larger diblock copolymer to the smaller copolymer). Taken together with other studies,[12−17] several key findings were established for the case of symmetric diblock copolymers, where the pure component diblocks form the lamellar morphology. First, the blends displayed complete miscibility (i.e., a single microphase separated lamellar morphology) when $R < 5$. For higher ratios of molecular weights, the blends were found to macrophase separate into nearly pure lamellar microdomains with different domain spacings, corresponding to the larger and smaller diblocks. Second, a miscibility gap opened up when the weight fraction of the larger diblock was less than 0.7 for $R > 7$ (in the range $5 < R < 7$, the miscibility gap was smaller). That is, at higher loadings of the smaller diblock, the blends showed two distinct microphase separated phases. Third, morphological transitions to a *cylindrical* morphology were seen upon blending at a particular composition and R value.[10]

In the present study we build and expand upon the earlier work. Specifically, we focus on blending lamellar-forming, high molecular weight *diblock* copolymers with a lamellar-forming, low molecular weight *triblock* copolymer. Only two previous studies have looked at blends containing triblock copolymers,[12,18] but with lower molecular weights and molecular weight ratios, $R < 4$. Here we employ diblock copolymers with molecular weights $M_n > 1 \times 10^5$ g/mol. This, coupled with the assertion that the triblock copolymer behaves morphologically as a diblock of half the molecular weight,[19] enables us to access molecular weight ratios in the range $14 < R < 43$ (here $R = M_n^{diblock}/{}^1/_2 M_n^{triblock}$), which are well beyond those previously reported ($R < 15$). In addition, use of the triblock allows us to probe the influence of polymer architecture on the behavior of the blends.

Experimental Section

Polymers. The high molecular weight diblock copolymers were synthesized by anionic polymerization under high-vacuum techniques, using glass reactors equipped with break-seals for the mixing of the reagents, and with constrictions for the removal of the products, as reported previously.[20] Styrene and isoprene monomers (Acros, 98%) were purified prior to polymerization, as described in detail elsewhere.[21] Benzene (Fluka 99%), the polymerization solvent, was carefully purified sequentially over CaH_2 and PS^-Li^+ and then stored under the latter. The initiator *sec*-BuLi (Aldrich, 1.4 M in cyclohexane) was used as received and diluted to lower concentrations in either hexane or benzene. Methanol (MeOH, Lab Scan, 99.8%) was dried over CaH_2 overnight under vacuum and was degassed twice before being distilled in precalibrated ampules. A typical synthesis began with the polymerization of

* Corresponding author. E-mail: elt@mit.edu.
[†] Massachusetts Institute of Technology.
[‡] University of Ioannina.

10.1021/ma801022k CCC: $40.75
Published on Web 07/16/2008

Table 1. Molecular Characteristics of the Block Copolymers

sample	$(\bar{M}_n)_{PS} \times 10^3$ [a]	$(\bar{M}_n)_{total} \times 10^3$ [a]	$(\bar{M}_w)_{total} \times 10^3$ [c]	PDI[b]	Φ_{PS}[d]	χN[f]	R[h]
SI450	212	438	460	1.05	0.47	470	14
SI700	351	715	751	1.05	0.49	760	23
SI1000	443	944[e]	1001[e]	1.06	0.44	1010	30
SI1500	613	1318[e]	1437[e]	1.09	0.43	1410	43
SIS[g]	13.5	62	65	1.05	0.41	34	

[a] MO in toluene at 35 °C. [b] SEC in THF at 35 °C. [c] Calculations are based on the equation $I^b = \bar{M}_w/\bar{M}_n^a$. [d] ^{1}H NMR in $CDCl_3$. Volume fraction based on ^{1}H NMR values using the equation vol %$(PS)_{copolymer}$ = wt %$_{PS}$ ρ_{PI}/(wt %$_{PS}$ ρ_{PI} + [100 − wt %$_{PS}$]ρ_{PS}) (ρ_{PS} = 1.06 g/mL, ρ_{PI} = 0.911 g/mL). [e] The total molecular weights for the samples SI1000 and SI1500 were calculated in combination with SEC/MO (calculating PS) and ^{1}H NMR (calculating volume fraction of PS). [f] The segregation strength was computed based on the equation $\chi = 33/T - 0.0228$ from ref 36. [g] Only the molecular weight profile of the purchased triblock was detemined using SEC. The volume fraction of PS is based on the manufacturer's reported weight fraction, and the PDI is that for the entire triblock copolymer. [h] R is the molecular weight ratio for each series of blends containing the respective high molecular weight diblock, i.e., $R = M_n^{diblock}/{}_1/{}_2M_n^{triblock}$.

styrene using *sec*-BuLi in 500 mL of benzene at room temperature for at least 24 h, followed by the addition of the appropriate amount of isoprene and left to react for another day. The polymerization was terminated by adding a small amount of MeOH (1 mL). The molecular weight and polydispersity of the copolymers were characterized by a combination of size exclusion chromatography (SEC) and membrane osmometry (MO), while the copolymer composition was determined through ^{1}H NMR spectroscopy.

The poly(styrene-*b*-isoprene-*b*-styrene) (SIS) triblock copolymer is a commercially available thermoplastic elastomer sold under the trade name Dexco 4411. The volume fraction of polystyrene is ~0.41 with a number-average molecular weight of 62 000 g/mol, which translates into a central poly(isoprene) (PI) block of 35 000 g/mol and two PS end blocks of 13 500 g/mol each. The block copolymer characteristics are summarized in Table 1.

Sample Preparation. A series of blends were prepared for each of the high molecular weight diblock copolymers with the lower molecular weight triblock. The four series of blends are labeled on the basis of the molecular weight of the large block copolymer, that is, SI450, SI700, SI1000, and SI1500. The blend compositions in weight percent SI were 5%, 10%, 25%, 50%, 75%, 90%, and 95%, for a total of 28 blend samples. A particular blend sample is identified by the series name (as above) and the composition in weight percent, with that of the diblock copolymer listed first. For example, SI450 95/5, refers to the blends of the 438 000 g/mol SI diblock copolymer containing 95 wt % of the diblock and 5 wt % of the SIS triblock. Additionally, neat films of the SIS triblock and the four SI diblocks were prepared. The films were cast in ceramic crucibles of 1.3 mL nominal volume from 1.4% (w/v) toluene solutions. The solutions were covered with glass coverslips and placed under a bell jar and then allowed to slowly evaporate over a period of about 2 weeks, yielding bulk films of ~0.5 mm thickness. In order to promote near-equilibrium structures, the films were subsequently annealed at 125 °C for 72 h under vacuum.

Transmission Electron Microscopy. Thin film cross sections, in the range of 50−100 nm thickness, were obtained by sectioning at −100 °C on a Leica EM UC6 microtome equipped with the EM FC6 cryogenic stage. The samples were then exposed to osmium tetroxide (OsO_4) vapor, which preferentially stains the PI domains and is used as a contrast agent. The cross sections were then imaged in bright field in a JEOL 2011 transmission electron microscope (TEM) operating at 200 kV.

Ultra-Small-Angle X-ray Scattering (USAXS). Scattering profiles for the blend films were collected using an advanced Bonse-Hart instrument on the 32ID-B beamline at the Advanced Photon Source at Argonne National Laboratory using high intensity X-rays with a wavelength $\lambda = 0.10419$ nm. The data, consisting of absolute intensity as a function of scattering vector q ($q \equiv (4\pi/\lambda)\sin(\theta/2)$, where θ is the scattering angle), were corrected for background and analyzed by fitting model slit-smeared data to the intensity profiles. The data were also analyzed by desmearing the slit-smeared scattered intensity using an implementation of the standard method of Lake[22] included in the data reduction tools ("Indra") provided by Dr. Jan Ilavsky of the Advanced Photon Source.

Results

TEM analysis reveals, as expected, that all the neat block copolymers, having near-symmetric composition, form the lamellar structure in the bulk state (data not shown) and is corroborated by the scattering data. The TEM images of the various blend series are shown in Figures 1–3. As a general observation, the majority of the blends exhibit macrophase separation into two distinct morphologies, and the presence of the two kinds of microdomains is also evident in the scattering profiles, shown in Figures 4–7. Thus, the reflections from the diblock occur at lower q values, with multiple reflections from the triblock appearing at higher q, the strength of these scattering peaks depending upon blend composition. In the case of the SI450 and SI700 blends (images of the latter not shown), the behavior is very similar, and all blend samples exhibit solely the lamellar morphologies of the original block copolymers, with the exception of SI700 5/95, where PS cylinders in a PI matrix, in addition to thin lamellae and thick lamellae, were observed (Figure 1h). In this instance, however, the USAXS data indicate a predominantly lamellar−lamellar morphology (Figure 5), suggesting that only a small volume percent of isolated islands of cylinders exist. In the case of the two higher molecular weight diblock blends (SI1000 and SI1500), the macrophase separation is accompanied by the appearance of nonlamellar morphologies in a wide range of compositions (see Figures 2 and 3).

The shift of the first-order scattering peak (q_1) with increased SIS loading provides a means of tracking the change in domain spacing of the high molecular weight diblock-rich phase (Figure 8). For all the blends studied, the domain spacing of the diblock-rich phase decreases upon addition of the triblock until a saturation point is reached, and thereafter the domain spacing remains relatively unchanged. This decrease in domain spacing upon addition of a suitable surfactant-like modifier is well-known and arises as a result of the localization of the triblock at the intermaterial dividing surface (IMDS) between the two high molecular weight blocks, effectively increasing the interface area per unit volume and leading to chain relaxation near the interface.[6,23] On the other hand, the domain spacing of the triblock rich phase remains constant throughout, indicating very little solubility of the large diblocks in the triblock. A final observation from the scattering data, specifically for the SI450 and SI700 blends, is that the long-range order of the diblock-rich domains appears to improve with added triblock, as evidenced by the sharper and more pronounced low-q scattering peaks. It is presumed that this arises from the shrinking size of the diblock phase regions as their volume fraction decreases, thereby leading to an enhanced effect of the phase boundaries to "template" the ordering, in analogy to the commensurate ordering of block copolymers in troughs reported previously by our group.[24] Additionally, the added triblock copolymer could be acting as a plasticizer for the diblock domains, reducing the glass transition temperature, and diluting the entanglement networks of both the PS and PI domains, thus allowing for

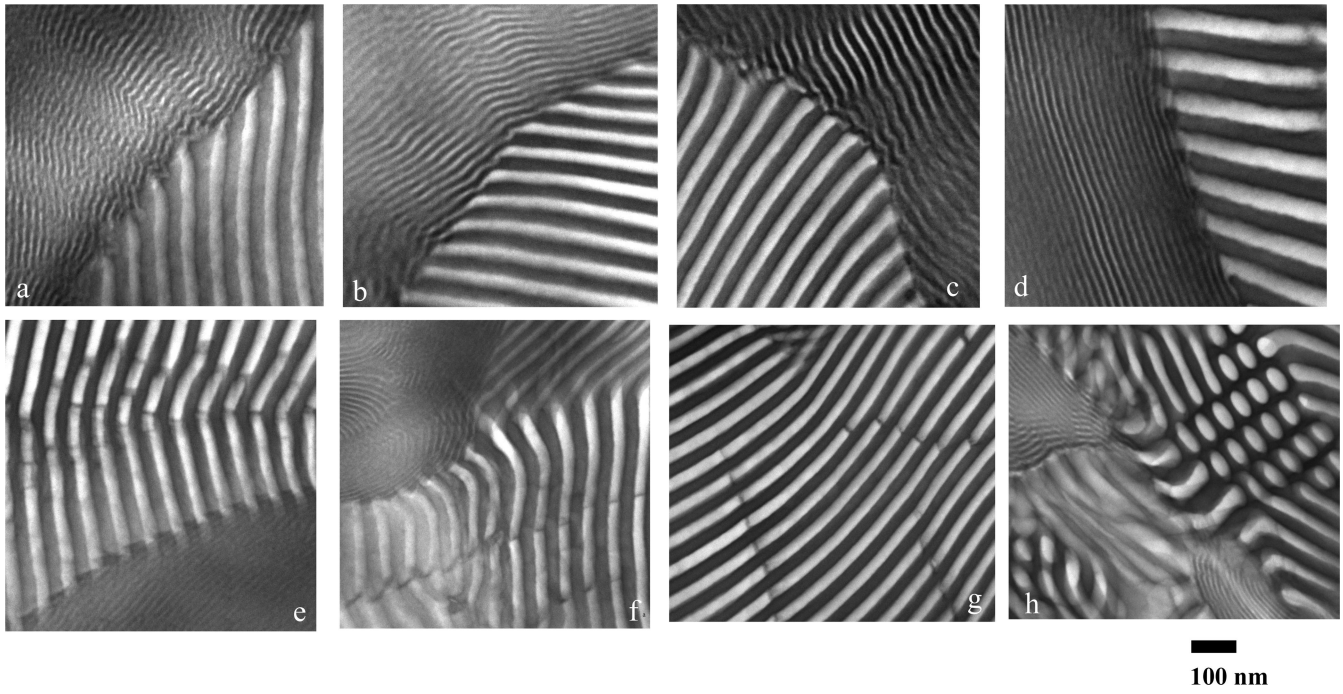

Figure 1. Bright field TEM micrographs of thin OsO_4-stained sections of blends of SI450 with SIS, with compositions in weight percent (SI450/SIS): (a) 5/95, (b) 10/90, (c) 25/75, (d) 50/50, (e) 75/25, (f) 90/10, (g) 95/5, (h) the exceptional SI700 5/95 blend exhibits some cylindrical domains in the minority SI700 phase in addition to thick and thin lamellar regions. Note that the micrographs were taken from areas containing both the thin triblock lamellae and thick diblock lamellae, to indicate the coexistence of the two phases, and are not representative of the actual volume percent of each type of domain, which varies strongly with blend composition.

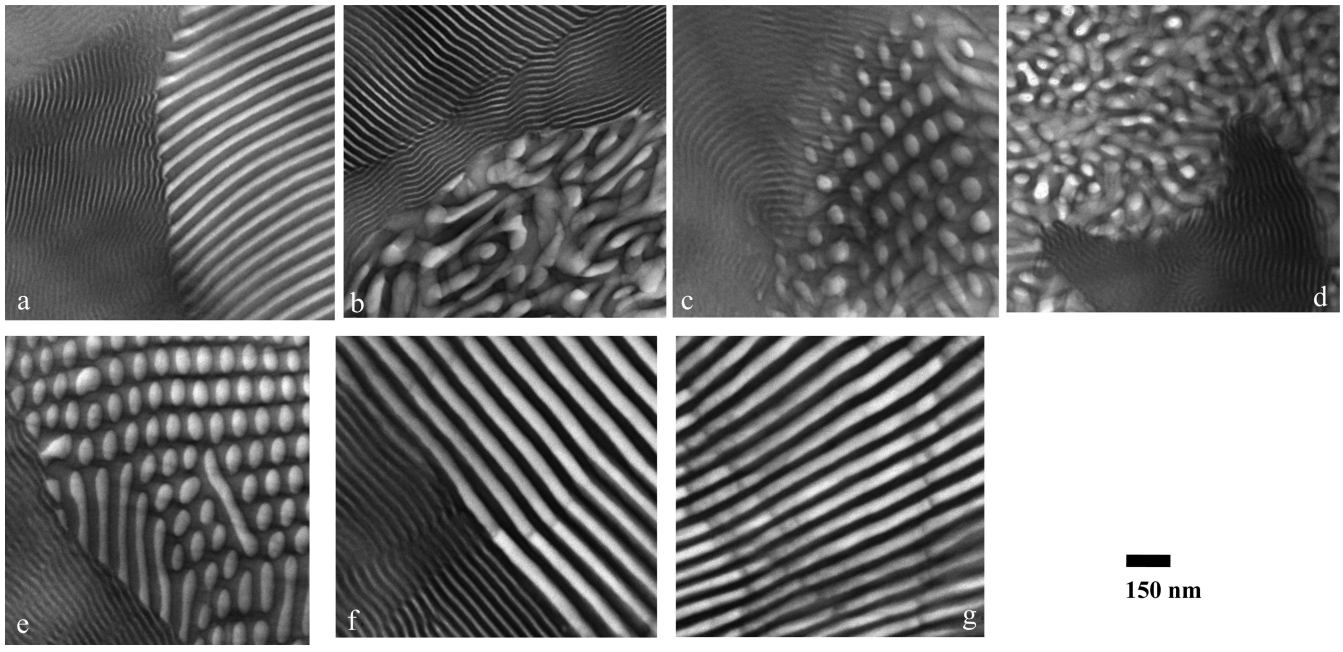

Figure 2. Bright field TEM micrographs of thin OsO_4-stained sections of blends of SI1000 with SIS, with compositions in weight percent (SI1000/SIS): (a) 5/95, (b) 10/90, (c) 25/75, (d) 50/50, (e) 75/25, (f) 90/10, (g) 95/5. The 10/90 and 50/50 blends exhibit a disordered morphology with IMDS curvature toward the PS domains, whereas the 25/75 and 75/25 blends reveal a PS cylindrical morphology. According to the scattering data, the 10/90 blend appears to be disordered cylinders, whereas the 50/50 blend could be double gyroid, but it is not entirely clear. Nonetheless, micrographs for the latter blend suggest a bicontinuous morphology.

enhanced mobility of the chains.[25] It is also noteworthy that the diblock-rich domain spacing begins to plateau at around 25 wt % addition of the triblock, which is likely a good estimate of the solubility limit of the triblock in the diblock.

Discussion

Based on the microscopy and scattering data, a morphological phase diagram in the parameter space of molecular weight ratio (R) and composition was constructed and is shown in Figure 9. As mentioned previously, the molecular weight ratio was computed on the basis of the assumption the triblock copolymer behaves morphologically as a diblock of half the molecular weight.[19] There are two key features of note in the phase diagram. First, all the blends become multiphased in the weight fraction range of SI, $w_{SI} < 0.9$. That is, the blends phase separate into two distinct types of microdomain structures, one of which

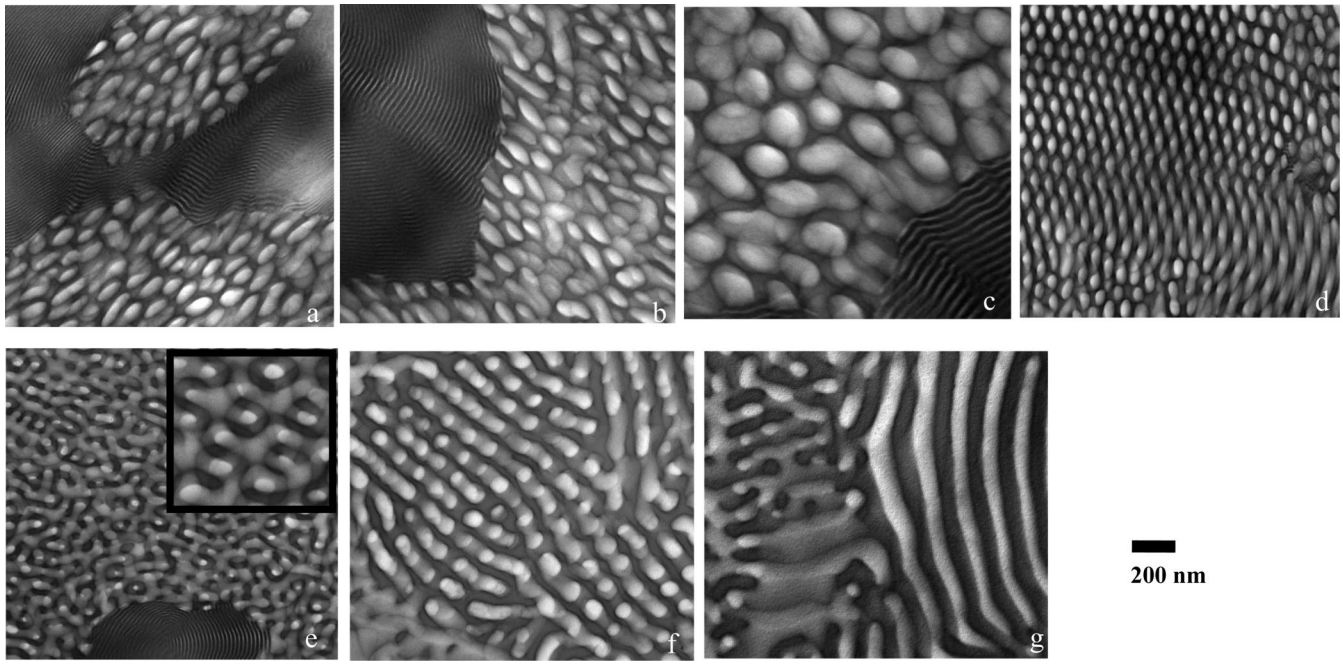

Figure 3. Bright field TEM micrographs of thin OsO_4-stained sections of blends of SI1500 with SIS, with compositions in weight percent (SI1500/SIS): (a) 5/95, (b) 10/90, (c) 25/75, (d) 50/50, (e) 75/25, (f) 90/10, (g) 95/5. The 5/95, 10/90, and 25/75 blends exhibit a disordered morphology, which once again appears from the scattering data to be cylinders. The 75/25 blend appears to exhibit a poorly ordered double-gyroid structure, and a detail of the structure, showing characteristic serpentine features, is shown in the inset of (e). Note that while the effective volume fraction of the blends remains in the lamellar region of the phase diagram ($0.41 < \Phi_{PS}^{eff} < 0.44$), the IMDS is nonflat, with curvature toward the PS domains.

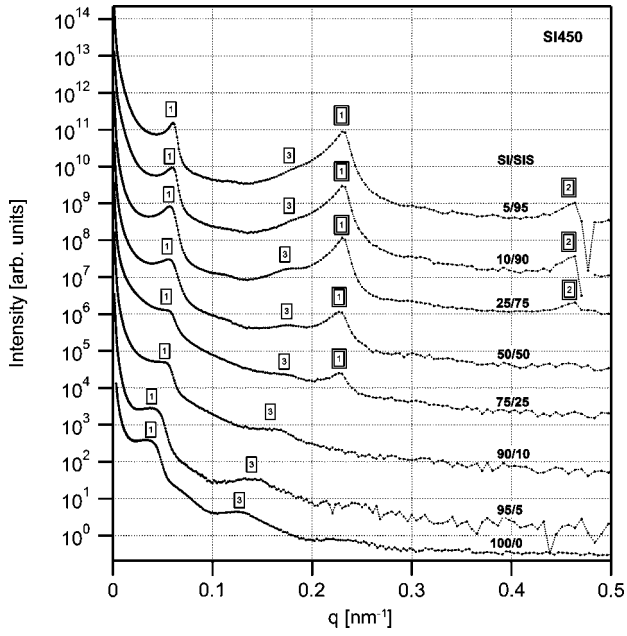

Figure 4. USAXS profiles for the SI450 series of blends. The lamellar reflections from the two different phases are clearly evident, with the intensities of the SIS triblock reflections increasing with the weight fraction of the triblock in the blend. A single box outline indicates reflections from the diblock domains and a double box those of the triblock domains.

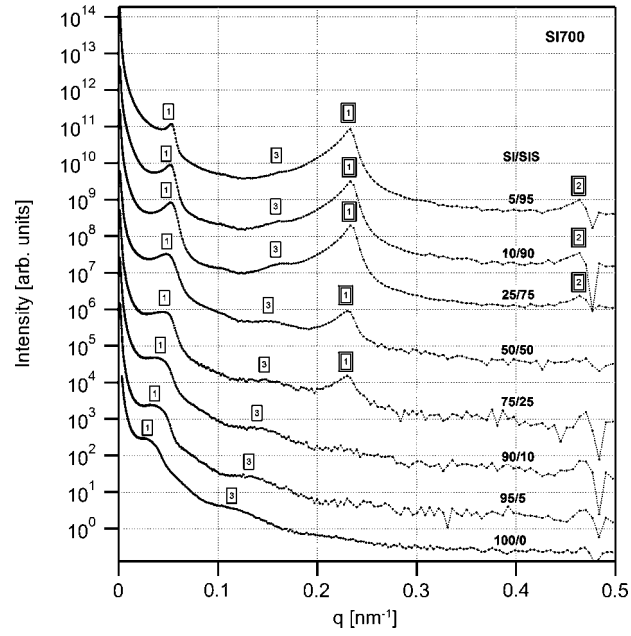

Figure 5. USAXS profiles for the SI700 series of blends, which are qualitatively similar to those of the SI450 blends. A single box outline indicates reflections from the diblock domains and a double box those of the triblock domains.

is always the lamellar-structured SIS triblock. This macrophase separation has been observed before in previous studies[3–5,7,13] and was attributed to the initial onset of microphase separation of the larger block copolymer upon solvent evaporation.[4] Nonetheless, in the present investigation, the miscibility gap is larger than that reported in the earlier studies, where the block copolymers were found to be immiscible for a weight fraction range of the large copolymer, $w_{large} < 0.7$.[10] This is undoubtedly linked to the much larger mismatch in the molecular weights of the diblocks with respect to the triblock in the present study and implies that the former is virtually insoluble in the latter. This larger miscibility gap was predicted in a theoretical study of block copolymer blends by Matsen.[26] This study presented two phase diagrams, for $R = 10$ and 25 and up to $\chi N_{large} = 600$ (cf. Figure 2 in ref 26). The phase diagrams showed that for blends where the interaction parameter and molecular weight ratio are large, as is the case in the present study (e.g., $\chi N_{large} \sim 700$ and $R \sim 25$ for the series of SI700 blends), the blends

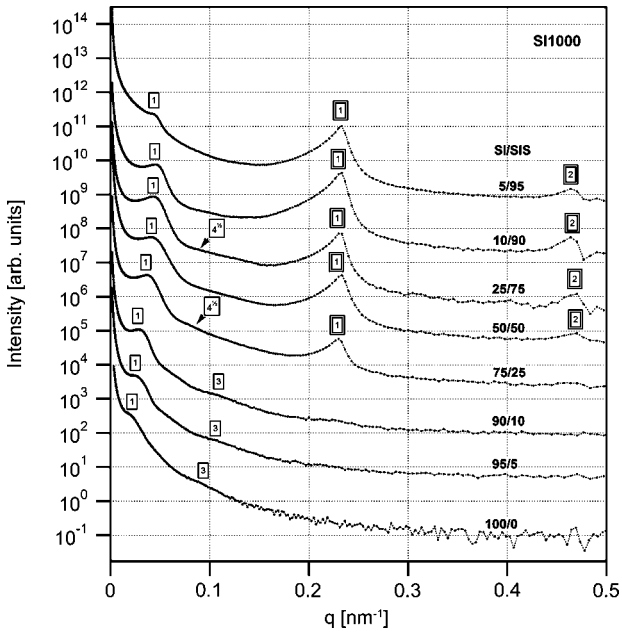

Figure 6. USAXS profiles for the SI1000 series of blends. The higher order peaks of the large diblock are weak or absent, indicating poor long-range order. A single box outline indicates reflections from the diblock domains and a double box those of the triblock domains.

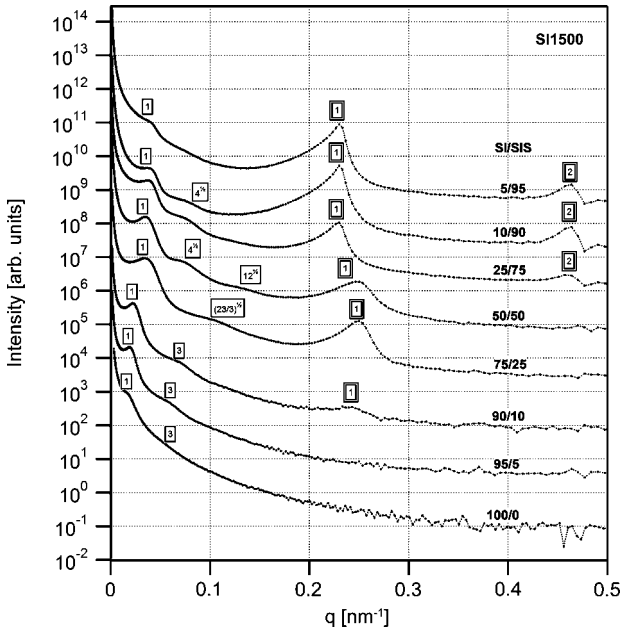

Figure 7. USAXS profiles for the SI1500 series of blends. The change in the scattering profile going from 25% SIS to 50% SIS is clearly evident, indicating a change in the morphology from double-gyroid-like to cylinders. A single box outline indicates reflections from the diblock domains and a double box those of the triblock domains.

become immiscible when $w_{large} < 0.85$, in close agreement with our experimental results.

The second notable feature is that morphological transitions (i.e., to nonlamellar morphologies) begin to appear in the SI majority phase at $R \sim 30$. Compared to the consolidated phase diagram previously presented by Yamaguchi and Hashimoto,[10] where a two-phase region begins at $R \sim 7$ and is assumed to extend beyond $R > 15$, here we find no morphological transitions in the range $10 < R < 30$ (with the single exception of the SI700 5/95 blend). Moreover, though morphological transitions have been reported previously,[3,7,10] these were restricted to the formation of the cylindrical microstructure.[27] In the present study, in addition

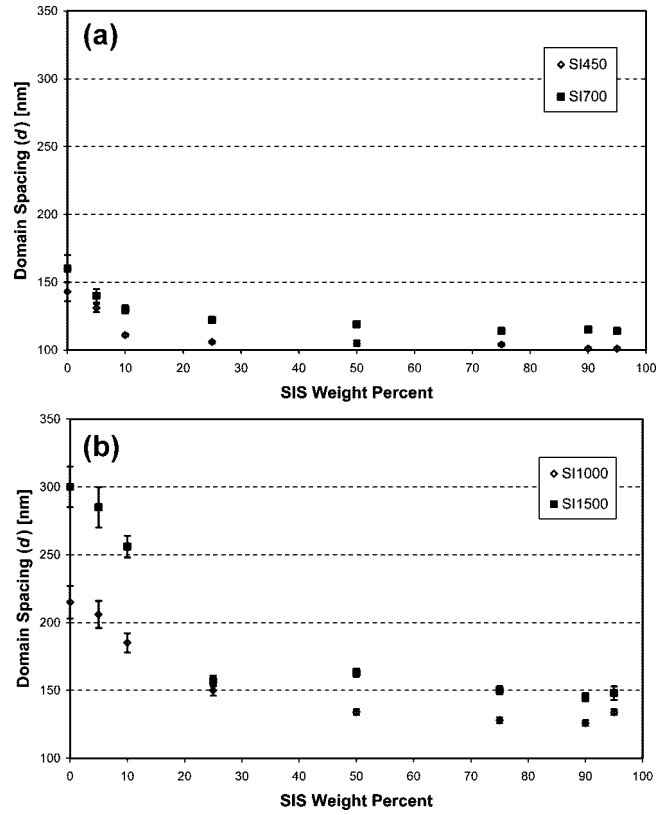

Figure 8. Domain spacing ($d = 2\pi/q_1$) as a function of the triblock content for the (a) SI450 and SI700 blend series and (b) for the SI1000 and SI1500 blend series, obtained by tracking the position of the first-order reflection in the USAXS data. The domain spacing decreases with increased triblock content and levels off after around 25 wt %.

to hexagonally packed PS cylinders (Figures 2c,e and 3d), a disordered or wormlike cylindrical (PS) phase (Figures 2b,d and 3a−c) and a bicontinuous phase resembling the double gyroid (Figure 3e) are observed. As a direct result of the very high molecular weights of the diblock copolymers, the SI1500 and especially the SI1000 blend samples show rather poor long-range order in TEM images and in USAXS, as evidenced by the broad peaks and weak (or absent) higher-order reflections (Figures 6 and 7). The USAXS data are largely consistent with the microscopy observations, with characteristic scattering peak ratios at 1 and $\sqrt{4}$ present in the SI1500 scattering results (as well as $\sqrt{12}$ in SI1500 50/50), substantiating the characterization of these samples as having the cylindrical morphology in the diblock-rich phase. For the SI1000 blends (10/90, 25/75, and 75/25), though the low-q scattering data show essentially one peak, a thorough analysis of many TEM micrographs and comparison to the SI1500 TEM data allows for the assignment of the cylindrical morphology to these samples with a high degree of certainty.

In the blend sample exhibiting the presumed double-gyroid morphology, SI1500 75/25, the scattering data show two distinct peaks, with peak ratios of 1 and ~2.75, which is inconsistent with a cylindrical morphology but coincides with the {631} reflection of the double gyroid [$(23/3)^{1/2} \approx 2.77$]. Furthermore, the disappearance of the peak at $\sqrt{4}$, evident in the neighboring blend sample (SI1500 50/50) which shows the cylindrical morphology, requires the assignment of another, noncylindrical, morphology to this blend. The TEM micrograph (Figure 3e) of this blend is reminiscent of the double-gyroid morphology and extends over large areas (see Supporting Information). The morphology is clearly disordered, resulting in only a few broad scattering peaks, which do not allow for conclusive definition of the blend morphology. Nonetheless, taken together, the data suggest that

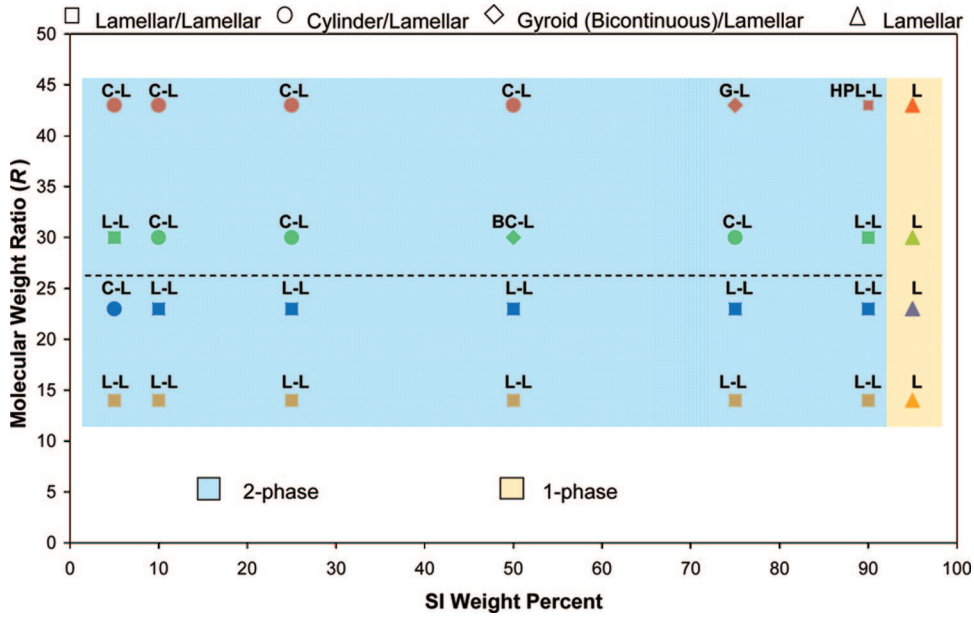

Figure 9. Morphological phase diagram of the binary blends in the parameter space of molecular weight ratio, $R = M_n^{diblock}/{}^1/_2 M_n^{triblock}$, and blend composition, in weight percent SI (to facilitate comparison with previous studies). The data points for each blend series are depicted in a unique color. The yellow shaded area represents the region where the blends are miscible and exhibit a single microphase separated morphology, whereas the blue shaded area indicates the macrophase separated region with two coexisting microphase separated morphologies. Above the dotted line, morphological phase transitions are observed, from lamellar arrangement to structures with IMDS curvature, i.e. cylinders and double-gyroid-like, identified by different data point shapes on the graph.

the observed morphology is likely double gyroid. With respect to the stability of this phase, the sample was annealed for an extra 7 days with no change observed in the scattering, indicating that the morphology is likely not kinetically trapped. The observation of this double-gyroid-like phase, which was not reported in previous studies on blends of diblock copolymers, is not only appealing from a strictly morphological perspective but also lends further evidence as to the stability of the double-gyroid phase in block copolymer melts in general at high segregation strengths.[28–30]

Since the effective volume fraction of the blends remains within the lamellar region of the phase diagram, Yamaguchi and Hashimoto ascribed the morphological transitions into curved IMDS morphologies, to the influence of the asymmetric composition of the lower molecular weight block copolymer, which prefers a spontaneous nonzero curvature at the IMDS between the dissimilar blocks. They argued that in the neat lower molecular weight copolymer this small value of interface curvature would promote large radius domains, inconsistent with chain packing considerations, and hence the resulting neat morphology is lamellar. However, upon addition of a second, higher molecular weight block copolymer, the preferred nonflat curvature of the IMDS can be realized, since the larger block copolymer chains can fill the extra space required to accommodate the small nonzero spontaneous curvature (cf. Figure 14 in ref 10).[7,10] It is evident then that, for a small compositional asymmetry in the lower molecular weight block copolymer, higher values of R (i.e., longer chains of the large block copolymer) would be required to induce the nonflat IMDS morphologies by allowing the formation of larger radius structures. This is precisely what is observed in the present study. As in the prior work, the overall volume fraction of the blends here would indicate a lamellar morphology in the diblock-rich phase (Φ_{PS} in the range 0.41−0.44); nonetheless, as the molecular weight of the diblock increases, curved IMDS morphologies appear in the blends composed of SI1000 and SI1500. Also noteworthy is that the size of the cylindrical domains stays relatively constant in the blends, as evidenced by the roughly constant domain spacing in the blends with a cylindrical morphology (see Figure 8b).[31] Since the spontaneous curvature is expected to be determined by the mismatch in size of the respective blocks in the triblock, which is constant, this lends further support to the explanation for the appearance of cylindrical domains resulting from an expression of a spontaneous curvature, as outlined above.

Despite experimental observations, prior theoretical studies have not predicted this morphological transition in nearly symmetric block copolymer blends, with the exception of the strong segregation limit (SSL) theory of Lyatskaya et al., where a lower free energy for the cylindrical morphology was found in a certain composition window with $w_{large} \leq 0.4$ for two lamellar-forming diblock copolymers.[32] However, the composition of one of the two diblocks was rather asymmetric (nearly cylinder-forming), and the molecular weight ratio was $R \leq 2$. Yamaguchi et al. applied this model in their study and were unable to demonstrate that the cylindrical microstructure is favored over the lamellar microstructure in their blends.[7] The self-consistent field theory (SCFT) study by Matsen[26] focused on selected values of χN and R, and although it demonstrated the macrophase separation into two coexisting lamellar phases, no cylindrical domains were reported. Shi and Noolandi utilized the SCFT to map out a phase diagram ("phase cube") for a pair of diblocks of equal length (i.e., $R = 1$) and found interesting changes in the phase diagram, but again their work did not predict phase transitions to curved IMDS structures when the effective volume fraction of the blends was near 0.5, unless one of the diblocks was highly asymmetric (i.e., nearly a homopolymer).[33] In another study, Shi and Noolandi investigated the effects of short diblocks (effectively non-ordering surfactants) on the phase behavior of strongly segregated long diblocks ($R = 10$),[34] and two of their findings are of note in the present context. First, when their composition was near 0.5, a sizable proportion (~20%) of the short diblock chains tended to segregate to the interface between the large diblock domains, acting as surfactants. This is near the estimated value of ~25% for the solubility limit of the triblock in the domains of the large diblock in this study.

Second, the chain end distribution of the long diblock was found to deviate from the analytical SSL theory of Semenov,[35] with the chain end density increasing gradually from the interface to the center of the domain. This hints at the possibility of chain end effects playing a role in determining the microstructure. In the case of the SSL theory of Lyatskaya et al., the chains are presumed to be highly stretched, and the long diblock chain ends are explicitly excluded from folding back and mixing with the short diblock segments near the interface.[32] That the long diblock copolymer chains could be folding back on themselves inside the cylindrical domains is supported by our data, where the cylinder radius is much smaller than the length of the high molecular weight chains in the lamellar domains (see Figure 8).[31] It seems logical that in order to best fill the cylindrical space the long diblock chains would fold back toward the cylinder IMDS to maintain constant segmental density and to avoid overcrowding in the center of the cylinder. It would be of great interest to have SCFT studies in the relevant composition range, which account for chain segment distribution, in order to compare to the experimental results and assess whether this hypothesis is correct.

The strongly segregating high molecular weight diblock copolymers used in this study, having very high χN values, allowed for the exploration of the phase space that was not accessed in previous studies. Additionally, the higher absolute molecular weights of the diblocks contributed to an increased miscibility gap and permitted the extension of the morphological phase diagram for molecular weight ratios $R > 15$. It remains to be seen in follow-up studies whether these factors influenced the morphology of the blends. In particular, it is of interest to investigate blends where $R < 5$, but the absolute molecular weights are large ($M_n \sim 1 \times 10^6$ g/mol). In previous studies, blends with $R < 5$ were miscible at all compositions, but the increased molecular weights and segregation strength of the two components could lead to phase separation and/or morphological transitions. It is also important to determine whether chain architecture influences the observed morphology. In the current study, we postulate that the morphology of the neat triblock is equivalent to that of a diblock of half the molecular weight, as was demonstrated previously,[19] and it is on this basis that the molecular weight ratio, R, is calculated. Nonetheless, the connectivity of the blocks is a factor for the morphology of the blends, possibly influencing the nature of the morphological transitions and the solubility of the block copolymers. For instance, it is clear that bridges are not possible for the triblock in the large molecular weight diblock, since the PI middle block would not be able to span the large domain sizes present in the diblock. As such, only midblock loops or homogeneous solubility of the triblock in the diblock are possible. It is interesting to consider the possibility that the connectivity of the triblock (as opposed to diblock) copolymer could be favoring the formation of 3-D bicontinuous structures with nonzero mean curvature over the 2-D cylindrical structure, and this also forms the basis of future studies.

Conclusion

A series of blends of high molecular weight diblock copolymers with a lower molecular weight triblock copolymer were prepared and their morphological characteristics expressed on a phase diagram in the parameter space of molecular weight ratio and blend composition. Molecular weight ratios in the range $14 < R < 43$ were accessed, considerably extending the range previously studied. The observed blend morphologies shared many of the same features previously reported, including miscibility gaps with macrophase separation into two distinct microphase separated domains and morphological transitions from lamellar to cylindrical structures. Additionally, disordered bicontinuous and double-gyroid-like structures were also observed at certain compositions. The change from the flat zero curvature IMDS of the lamellar morphology to curved IMDS structures was presumed to result from compositional asymmetry of the block copolymers (Φ_{PS} in the range 0.41−0.44) and the preference for a nonzero IMDS curvature in the SIS triblock. The phase diagram showed a narrow region of complete miscibility, for $w_{SI} > 0.9$, in line with theoretical studies.[26] Future studies will focus on the role of the high absolute molecular weights, as well as chain architecture, on the morphological behavior of the blends.

Acknowledgment. This work was supported by a grant from the U.S. Air Force Office of Scientific Research (AFOSR #FA9550-05-1-0056) and partially carried out at the MIT Institute for Soldier Nanotechnologies (ISN). This work also made use of the Shared Experimental Facilities supported by the Center for Materials Science and Engineering at MIT, as part of the MRSEC Program of the National Science Foundation under Award DMR 02-13282. The USAXS data were acquired at the Advanced Photon Source at Argonne National Laboratory, and special thanks are extended to Dr. Jan Ilavsky for his invaluable assistance with data collection, reduction, and modeling. Use of the Advanced Photon Source was supported by the U.S. Department of Energy, Office of Science, Office of Basic Energy Sciences, under Contract DE-AC02-06CH11357. We also thank Prof. Chinedum Osuji for collecting SAXS data on some samples for comparison with the USAXS data obtained at Argonne National Laboratory. We are also indebted to Dr. Alfredo Alexander-Katz for enlightening discussions.

Supporting Information Available: Additional TEM images of the SI1500 75/25 blend, showing characteristic projections of a gyroid-like morphology over wide areas. This material is available free of charge via the Internet at http://pubs.acs.org.

References and Notes

(1) Ruzette, A. V.; Leibler, L. *Nat. Mater.* **2005**, *4*, 19–31.
(2) Hamley, I. W. In *The Physics of Block Copolymers*; Oxford University Press: New York, 1998; pp 331−412.
(3) Hashimoto, T.; Yamasaki, K.; Koizumi, S.; Hasegawa, H. *Macromolecules* **1993**, *26*, 2895–2904.
(4) Hashimoto, T.; Koizumi, S.; Hasegawa, H. *Macromolecules* **1994**, *27*, 1562–1570.
(5) Koizumi, S.; Hasegawa, H.; Hashimoto, T. *Macromolecules* **1994**, *27*, 4371–4381.
(6) Yamaguchi, D.; Bodycomb, J.; Koizumi, S.; Hashimoto, T. *Macromolecules* **1999**, *32*, 5884–5894.
(7) Yamaguchi, D.; Shiratake, S.; Hashimoto, T. *Macromolecules* **2000**, *33*, 8258–8268.
(8) Court, F.; Hashimoto, T. *Macromolecules* **2001**, *34*, 2536–2545.
(9) Court, F.; Hashimoto, T. *Macromolecules* **2002**, *35*, 2566–2575.
(10) Yamaguchi, D.; Hashimoto, T. *Macromolecules* **2001**, *34*, 6495–6505.
(11) Yamaguchi, D.; Hasegawa, H.; Hashimoto, T. *Macromolecules* **2001**, *34*, 6506–6518.
(12) Hadziioannou, G.; Skoulios, A. *Macromolecules* **1982**, *15*, 267–271.
(13) Papadakis, C. M.; Mortensen, K.; Posselt, D. *Eur. Phys. J. B* **1998**, *4*, 325–332.
(14) Kane, L.; Satkowski, M. M.; Smith, S. D.; Spontak, R. J. *Macromolecules* **1996**, *29*, 8862–8870.
(15) Lin, E. K.; Gast, A. P.; Shi, A. C.; Noolandi, J.; Smith, S. D. *Macromolecules* **1996**, *29*, 5920–5925.
(16) Floudas, G.; Vlassopoulos, D.; Pitsikalis, M.; Hadjichristidis, N.; Stamm, M. *J. Chem. Phys.* **1996**, *104*, 2083–2088.
(17) Almdal, K.; Rosedale, J. H.; Bates, F. S. *Macromolecules* **1990**, *23*, 4336–4338.
(18) Goldacker, T.; Abetz, V.; Stadler, R.; Erukhimovich, I.; Leibler, L. *Nature (London)* **1999**, *398*, 137–139.
(19) Hadziioannou, G.; Skoulios, A. *Macromolecules* **1982**, *15*, 258–262.
(20) Avgeropoulos, A.; Hadjichristidis, N. *J. Polym. Sci., Polym. Chem.* **1997**, *35*, 813–816.
(21) Uhrig, D.; Mays, J. W. *J. Polym. Sci., Polym. Chem.* **2005**, *43*, 6179–6222.

(22) Lake, J. A. *Acta Crystallogr.* **1967**, *23*, 191–194.
(23) Mayes, A. M.; Russell, T. P.; Deline, V. R.; Satija, S. K.; Majkrzak, C. F. *Macromolecules* **1994**, *27*, 7447–7453.
(24) Cheng, J. Y.; Ross, C. A.; Thomas, E. L.; Smith, H. I.; Vancso, G. J. *Adv. Mater.* **2003**, *15*, 1599–1602.
(25) Mader, D.; Bruch, M.; Maier, R. D.; Stricker, F.; Mulhaupt, R. *Macromolecules* **1999**, *32*, 1252–1259.
(26) Matsen, M. W. *J. Chem. Phys.* **1995**, *103*, 3268–3271.
(27) Although the statement is made of a gyroid (OBDD) structure observed in the blends described in ref 3, the data presented in that article is in fact more consistent with the cylindrical morphology. The TEM micrographs for the 50/50 and 80/20 blends (Figure 4) resemble cylindrical morphologies. Importantly, however, the SAXS data reveal the typical scattering peaks of the cylindrical morphology (in fact, the caption to Figure 9 labels them as "hexagonal" profiles, consistent with cylinders), indicating that this is the actual (or dominant) morphology. In a personal communication, the authors of the study confirmed that the majority of the structure was indeed cylinders, with some isolated areas of gyroid (OBDD). Furthermore, the composition of these blends varied with casting conditions, hinting that this is not a stable morphology.
(28) Urbas, A. M.; Maldovan, M.; DeRege, P.; Thomas, E. L. *Adv. Mater.* **2002**, *14*, 1850–1853.
(29) Davidock, D. A.; Hillmyer, M. A.; Lodge, T. P. *Macromolecules* **2003**, *36*, 4682–4685.
(30) Cochran, E. W.; Garcia-Cervera, C. J.; Fredrickson, G. H. *Macromolecules* **2006**, *39*, 2449–2451.
(31) Based on a 2-D model of hexagonal packing, the cylinder radius is directly proportional to the domain spacing, d, by the relation $r_{CYL} = d(2f/\sqrt{3}\pi)^{1/2}$, where f is the 2-D area ("volume") fraction.
(32) Lyatskaya, J. V.; Zhulina, E. B.; Birshtein, T. M. *Polymer* **1992**, *33*, 343–351.
(33) Shi, A. C.; Noolandi, J. *Macromolecules* **1995**, *28*, 3103–3109.
(34) Shi, A. C.; Noolandi, J. *Macromolecules* **1994**, *27*, 2936–2944.
(35) Semenov, A. N. *Sov. Phys. JETP* **1985**, *88*, 1242–1256.
(36) Lodge, T. P.; Pan, C.; Jin, X.; Liu, Z.; Zhao, J.; Maurer, W. W.; Bates, F. S. *J. Polym. Sci., Part B: Polym. Phys.* **1995**, *33*, 2289–2293.

MA801022K